3.3 Review of final focus designs for crab waist colliders

Anton Bogomyagkov, Eugene Levichev

Mail to: A.V.Bogomyagkov@inp.nsk.su

Budker Institute of Nuclear Physics (BINP),

Prospect Lavrentieva 11, Novosibirsk 630090, Russia

3.3.1 Introduction

Invention of the crab waist collision scheme promises increase of luminosity by several orders of magnitude for specially designed collider with respect to conventional. Successful test of the scheme at existent Italian lepton collider DAΦNE increased luminosity three times from 1.5×10^{32} cm^{-2}s^{-1} to 4.5×10^{32} cm^{-2}s^{-1} and proved the principle of crab waist. The moderate luminosity gain is due to limited possibility to implement all the necessary modifications. Hence, the projects of the new circular colliders exploit the crab waist interaction scheme. This review describes designs of interaction regions for already existent collider DAΦNE and SuperKEKB, for new projects of SuperB in Italy, CTau in Novosibirsk and FCC-ee in CERN. Designers of the new projects (FCC-ee, CEPC in China) continuously improve them; therefore, we describe only known to us present situation.

3.3.2 Crab waist collision scheme

P. Raimondi proposed crab waist collision scheme in 2006 [1]. Three founding steps are at the heart of crab waist collision scheme [2]. In order to understand these steps, we need expressions for luminosity L, horizontal ξ_x and vertical ξ_y tune shifts [3, 4]:

$$L \propto \frac{N\xi_y}{\beta_y^*},\ \xi_y \propto \frac{N\beta_y^*}{\sigma_x^*\sigma_y^*\sqrt{1+\varphi^2}},\ \xi_x \propto \frac{N}{\varepsilon_x\left(1+\varphi^2\right)}, \tag{1}$$

where N is bunch population, β_y^* is vertical beta function at the interaction point (IP), σ_x^*, σ_y^* and σ_z are horizontal, vertical and longitudinal beam sizes respectfully, using θ as a full crossing angle, Piwinski [5] angle is

$$\varphi = \frac{\sigma_z}{\sigma_x^*}\tan\left(\frac{\theta}{2}\right). \tag{2}$$

The first step is large Piwinski angle, which requires long bunches, small horizontal emittance, and a large crossing angle. This step reduces vertical tune shift and the size of interaction area (yellow on Figure 1). Therefore, one desiring to keep vertical tune shift unchanged increases bunch population and gains in luminosity. The

second step is reduction of the vertical beta function to half-length of the interaction region but not the bunch length. This again makes vertical tune shift smaller and luminosity larger. The third is introduction of the crab sextupoles at the proper phase advances from IP: $\Delta\mu_x = \pi \cdot m,\ \Delta\mu_y = \pi/2 \cdot (2n+1)$. The sextupoles rotate position of the vertical beta function waist along the axis of the opposite beam (Figure 2), and suppress betatron and synchrobetatron resonances [6, 7, 8, 9].

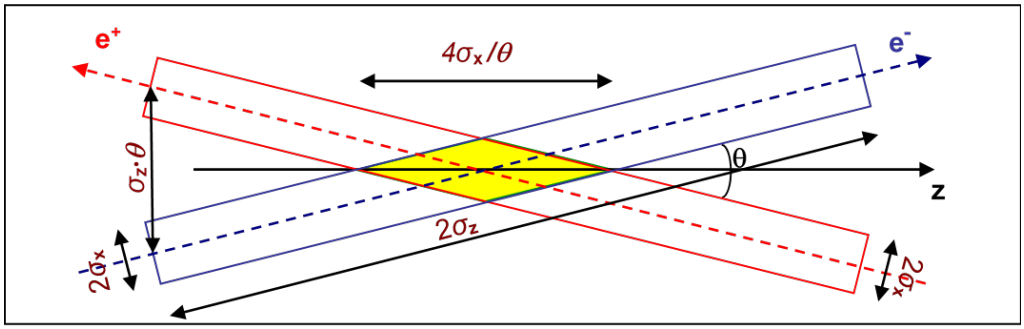

Figure 1: Layout of the crossing angle collision.

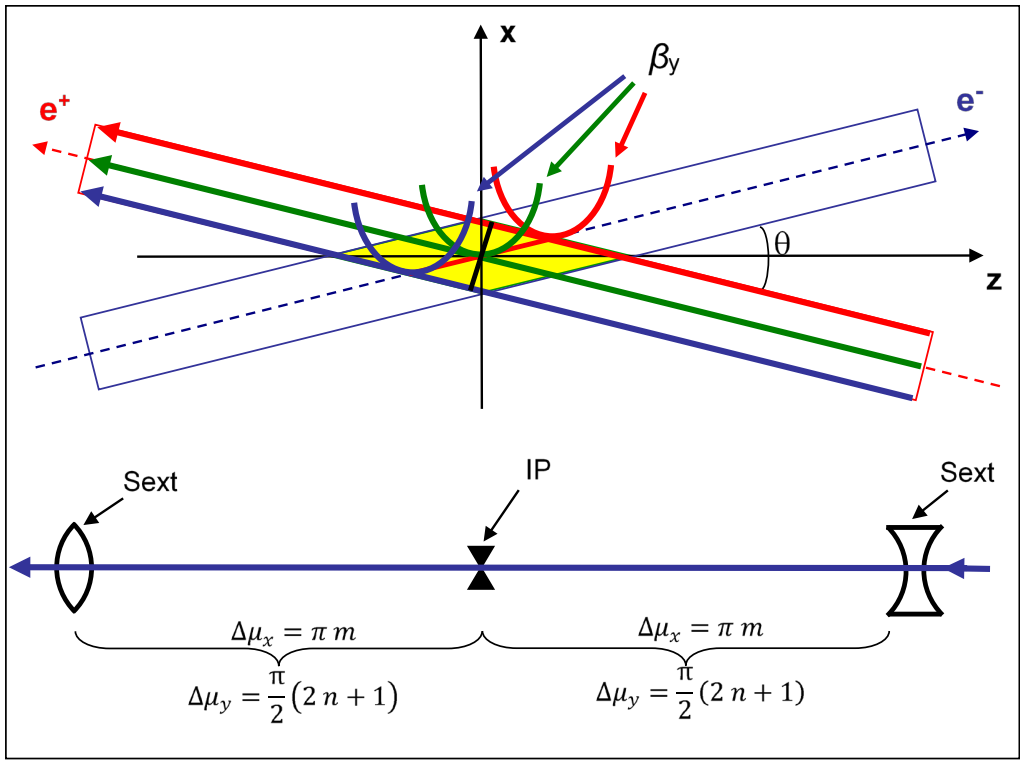

Figure 2: Crab waist collision scheme.

The integrated strength of the crab sextupoles at the place with vertical β_y and horizontal β_x beta functions is

$$K2L = \pm \frac{1}{\theta \cdot \beta_y^* \cdot \beta_y} \sqrt{\frac{\beta_x^*}{\beta_x}} . \qquad (3)$$

The crab sextupoles cancel each other's second order geometrical aberrations because of proper phase advances and appropriate sign of the field gradient promising no dynamic aperture degradation.

The requirements of the crab waist are

1. crossing angle,
2. bunch length, horizontal size and crossing angle should provide large Piwinski angle,
3. vertical beta function comparable with the size of the interaction area,
4. sextupoles with proper strength and phase advance from IP.

The actual exploitation of the crab waist scheme in accelerator could produce some difficulties:

1. small vertical beta function and desire to minimize beta functions in final quadrupoles, despite the crossing angle, might require double aperture quadrupoles with high gradient;
2. strong final quadrupoles with large beta function are the source of large chromaticity, and need local chromaticity correction sections;
3. chromaticity correction sections and final focus quadrupoles will produce large nonlinear chromaticity limiting energy acceptance of the ring;
4. small horizontal emittance increases chromaticity of the whole ring, and raises the strength of the sextupoles correcting it, and as a result abates dynamic aperture;
5. crab sextupoles require special phase advances from IP and beta functions to reduce the strength of sextupoles, which could be difficult or impossible in the upgrade of already operating collider;
6. interference between crab sextupoles and, if present, chromaticity correction sections might limit dynamic aperture.

3.3.3 **Nonlinear detuning**

For comparison of different interaction regions, we will introduce chromaticity produced by final defocusing quadrupoles (from both sides of IP, and final quadrupole could consist of several quadrupoles)

$$\mu'_y = \frac{1}{2}\sum_i K1L_i \cdot \beta_{i,y} \,, \tag{4}$$

where $K1L_i$ is integrated strength of i-th quadrupole, $\beta_{i,y}$ is vertical beta function in the centre of the i-th quadrupole.

Detuning coefficient of the vertical plane (α_{yy}) with respect to action J_y

$$\Delta\nu_y = \alpha_{yy}J_y + \alpha_{xx}J_x \tag{5}$$

is the simplest characteristic describing nonlinear properties of the lattice [10, 11]. It is not the accurate attribute: even if detuning (5) is small higher orders might reduce dynamic aperture. We will consider third order nonlinearities; therefore, the first order detuning allows comparison of different lattices. Since nonlinear effects are much stronger in vertical plane, we will omit estimations of the horizontal detuning. Assuming that FF quadrupole changes sign of Twiss functions α_y we derive the quadrupole integrated strength K1L [m^{-1}]

$$K1L \cdot L_q = -\frac{2}{L^* + L_q/2}, \tag{6}$$

where L_q is quadrupole length, L^* is the distance from IP to the face of the quadrupole.

Now we estimate chromaticity as

$$\mu'_y = -\frac{L^* + L_q/2}{\beta^*_y} \,. \tag{7}$$

From the Hamiltonian of the kinematic term

$$H = \frac{\left(P_x^2 + P_y^2\right)^2}{8}, \tag{8}$$

we decipher detuning coefficient for the drift between the FF quadrupoles

$$\alpha^k_{yy} = \frac{3}{16\pi}\int \frac{\left(1+\alpha_y^2\right)}{\beta_y^2} ds \approx \frac{3}{16\pi}\frac{L^* + L_q/2}{\beta^{*2}_y} \,. \tag{9}$$

Hamiltonian of the fringe field of FF quadrupole is

$$H = K1' \frac{\left(P_x xy^2 - P_y x^2 y\right)}{4} - K1'' \frac{\left(x^4 - y^4\right)}{48}, \tag{10}$$

and we obtain

$$\alpha_{yy}^{f} = \frac{1}{32\pi} \int K1'' \beta_y^2 ds \approx -\frac{1}{4\pi} \frac{K1 L^{*3}}{\beta_y^{*2}} \approx \frac{1}{2\pi} \frac{L^{*3}}{L_q \left(L^* + L_q/2\right) \beta_y^{*2}}. \tag{11}$$

The -I pair of sextupoles [11, 12] gives

$$\alpha_{yy}^{s} \approx -\frac{1}{16\pi} \left(K2 L_s\right)^2 L_s \beta_{s,y}^2, \tag{12}$$

where K2 is sextupole strength [m^{-3}], L_s is sextupole length, $\beta_{s,y}$ is vertical beta functions at the sextupole position.

3.3.4 **Present colliders: DAΦNE and Super KEKB**

3.3.4.1 ***DAΦNE***

DAΦNE is an electron-positron collider with central mass energy of 1.02 GeV (Φ resonance) delivering luminosity since 2000 [2]. The staff upgraded the machine to implement crab waist scheme in 2007. The changes included two times larger crossing angle, 26% smaller horizontal emittance, almost two times smaller vertical and horizontal beta functions, 50% smaller bunch length. Reduction of the bunch length was not intentional and happened because of continuous work on impedance reduction. Constraints of already working machine did not allow achieving extreme parameters; nevertheless, they doubled Piwinski angle from 0.8mrad to 1.7mrad (Table1) and increased luminosity three times [2].

Table 1: Parameters of DAΦNE and SuperKEKB

	DAΦNE	**SuperKEKB**	
	SIDDHARTA	LER	HER
Energy, GeV	0.51	4	7.007
Circumference, m	97.69	3016.315	
$\varepsilon_x/\varepsilon_y$, nm/pm	250/750	3.2/8.64	4.6/12.9
β^*_x/β^*_y, mm	250/9.3	32/0.27	25/0.3
Crossing angle, mrad	50	83	
σ_z, mm	17	6	5
Piwinski's angle φ	1.7	25	19
Beam current e^-/e^+, A	2.45/1.4	3.6	2.6
Beam beam tune shift ξ_y	0.03	0.088	0.08
μ'_y	-61	-5400	-5400
α^k_{yy}	694	1.8×10^6	1.8×10^6
α^f_{yy}	218	9.8×10^6	9.8×10^6
α^s_{yy}		-7×10^5	-7×10^5
Luminosity, $cm^{-2}s^{-1}$	Achieved 4.5×10^{32}	Design 8×10^{35}	

Moderate IP beta functions and small beta functions in final quadrupoles do not require separate chromaticity correction sections, and sextupoles of the ring correct the whole chromaticity. Figure 3 shows optical functions of DAΦNE interaction region.

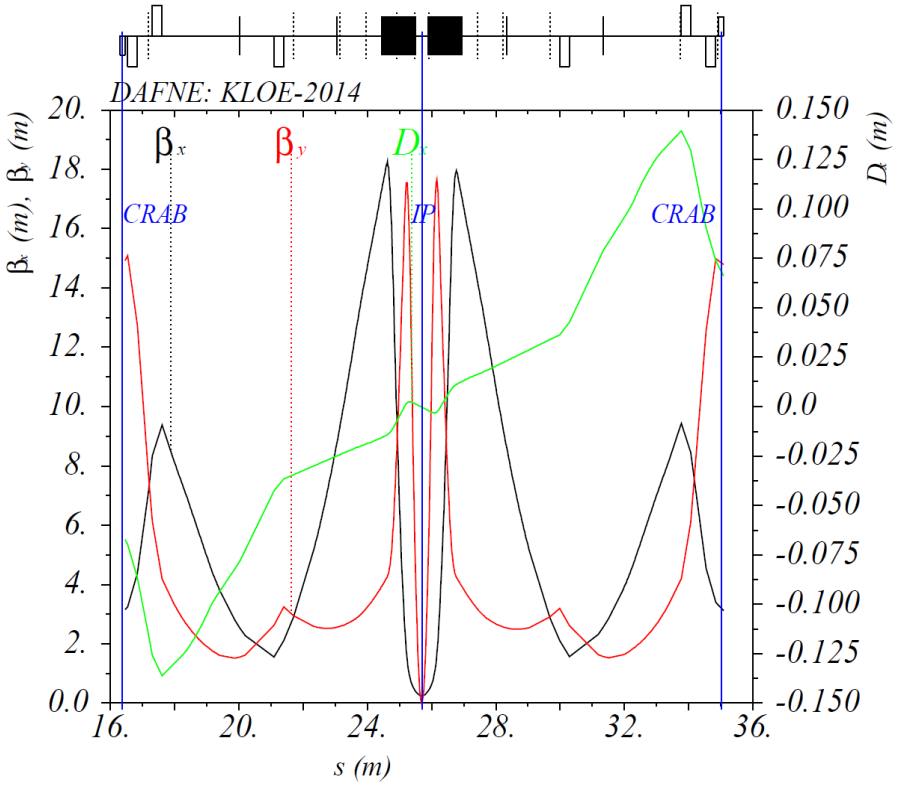

Figure 3: Optical functions of DAΦNE interaction region with crab waist sextupoles.

3.3.4.2 ***SuperKEKB***

SuperKEKB [13, 14, 15] is an upgrade of KEKB B-factory [13] in the state of beam commissioning [16] with the goal to increase luminosity 40 times to 0.8×10^{36} $cm^{-2}s^{-1}$ (Table 1). The upgrade followed the steps of crab collision scheme and, because of very small beam sizes at IP, received the name of nano-beam. Figures 5 and 6 show optical functions of the interaction region for low (LER) and high (HER) energy rings.

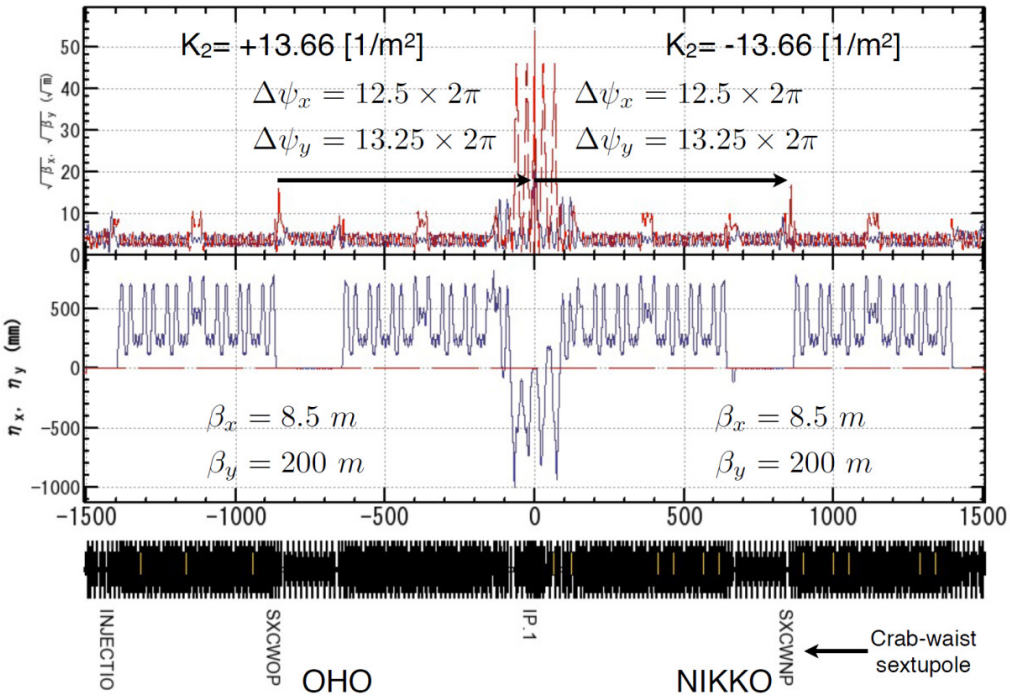

Figure 5: Optical functions of SuperKEKB LER interaction region with crab waist. sextupoles.

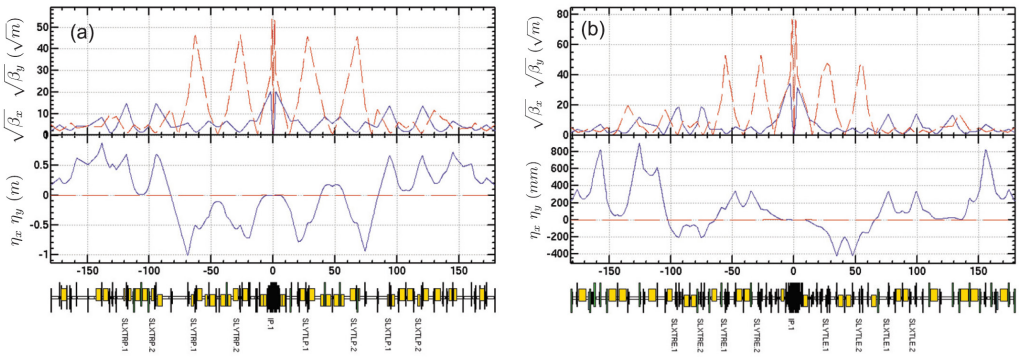

Figure 6: Optical functions of SuperKEKB interaction region (a) LER, (b) HER.

The crab sextupoles are installed before horizontal and vertical chromaticity sections, rather far from IP at $\mu_x = 12.5 \times 2\pi$ and $\mu_y = 13.25 \times 2\pi$. The interplay of crab sextupole, nonlinear fringe of final quadrupoles, and kinematic term in the IP drift reduces dynamic aperture drastically [17, 18] (Figure 7). The staff did not find a solution to regain dynamic aperture; therefore, they planned to work without crab sextupoles.

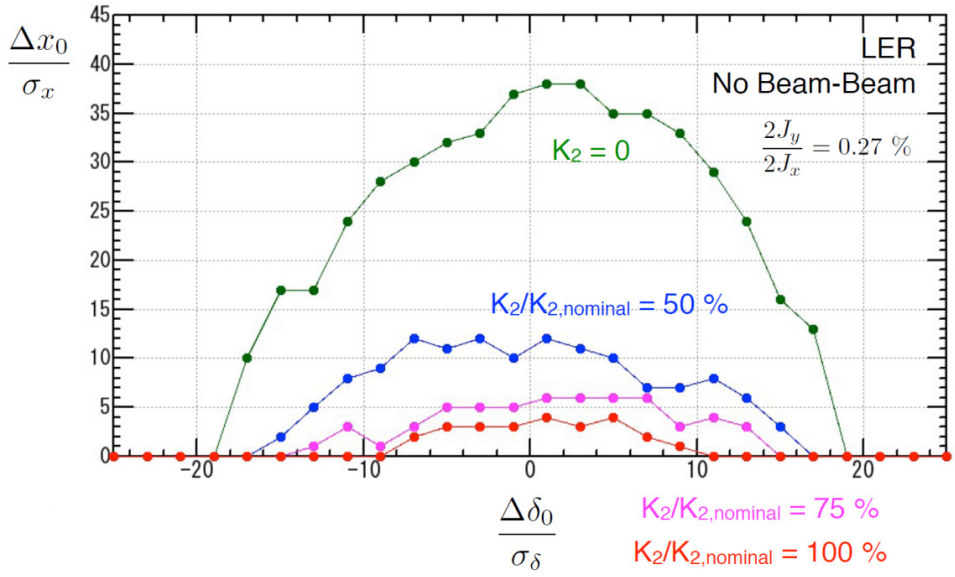

Figure 7: Dynamic aperture for LER SuperKEKB with different crab sextupole strength.

3.3.5 Future projects based on crab waist

3.3.5.1 *SuperB*

SuperB [19, 20] is an Italian project of asymmetric b factory employing crab waist collision scheme to achieve luminosity of 1×10^{36} $cm^{-2}s^{-1}$. The optics of the interaction region includes separate vertical and horizontal chromaticity correction sections followed by crab sextupole (Figure 8). Again, dynamic aperture shrinks under influence of crab sextupoles (Figure 9), but it is satisfactory.

Table 2: Parameters of SuperB

	SuperB	
	LER	HER
Energy, GeV	4.18	6.7
Circumference, m	1258.4	
$\varepsilon_x/\varepsilon_y$, nm/pm	2.46/6.15	2/5
β^*_x/β^*_y, mm	32/0.205	26/0.253
Crossing angle, mrad	66	
σ_z, mm	5	5

Piwinski's angle φ	19	23
Beam current, A	2.4	1.9
Beam beam tune shift ξ_y	0.097	0.097
μ'_y	-1068	-1056
α^k_{yy}	1×10^6	1×10^6
α^f_{yy}	2.8×10^5	2.8×10^5
α^s_{yy}	-5.4×10^6	-5.4×10^6
Luminosity, $cm^{-2}s^{-1}$	1×10^{36}	

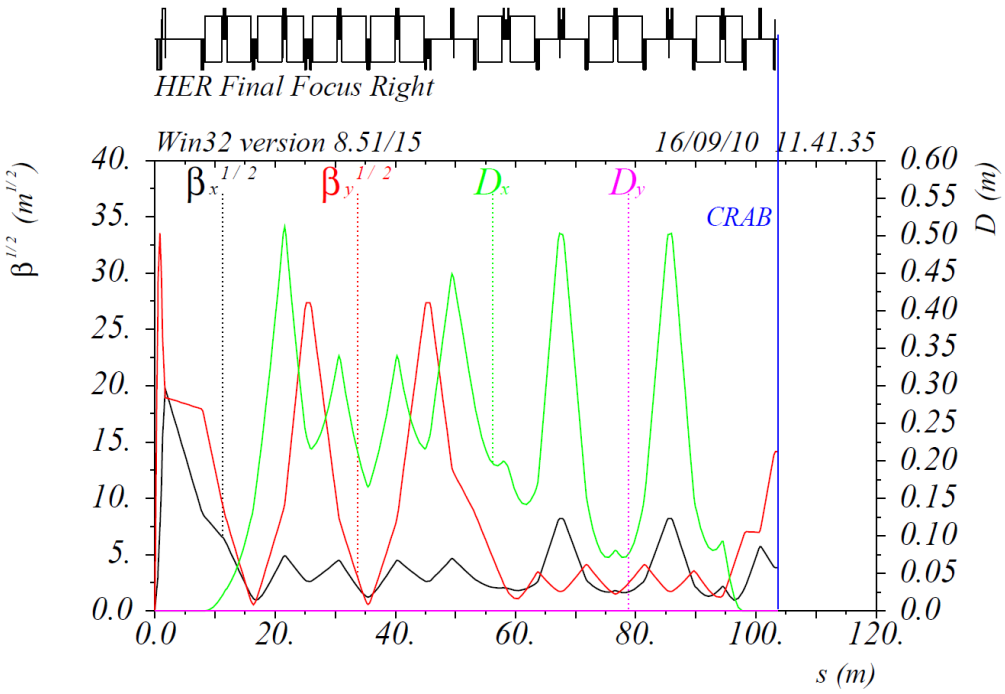

Figure 8: Optical functions of SuperB HER interaction region with crab waist sextupoles.

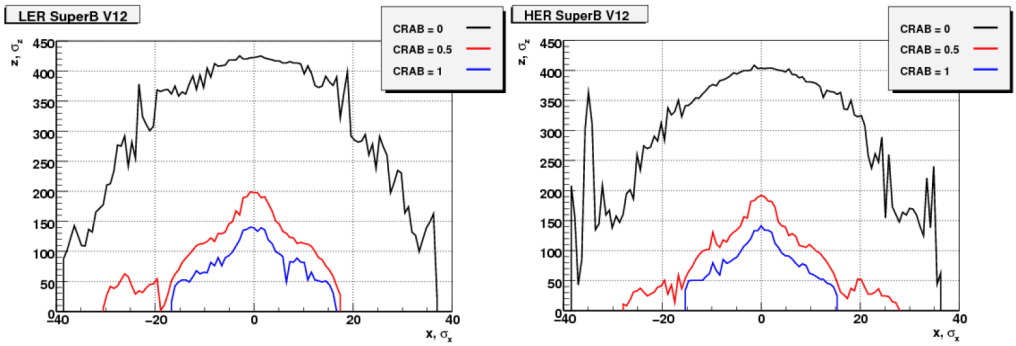

Figure 9: On momentum dynamic aperture of SuperB LER and HER: black line — crab sextupoles are off, red and blue — crab sextupoles strength of 50% and 100% of nominal respectfully.

3.3.5.2 *CTau*

Super Charm–Tau Factory is a project of electron-positron collider in the Budker Institute of Nuclear Physics (Novosibirsk, Russia) [21]. Designed center mass energy range of operation is from 2 to 5 GeV with luminosity reaching 1×10^{35} $cm^{-2}s^{-1}$(Table 3). It also relies on the crab waist collision scheme. China proposed similar project HIEPA [22].

Table 3: Parameters of CTau in Novosibirsk

	CTau			
Energy, GeV	1	1.5	2.0	2.5
Circumference, m	813.4			
$\varepsilon_x/\varepsilon_y$, nm/pm	8/40			
β^*_x/β^*_y, mm	40/0.8			
Crossing angle, mrad	60			
σ_z, mm	16.5	11	10	10
Piwinski's angle φ	27	19	17	17
Beam current, A	1.65			
Beam beam tune shift ξ_y	0.15	0.15	0.12	0.1
μ'_y	-697			
α^k_{yy}	1.3×10^5			
α^f_{yy}	7.7×10^5			
α^s_{yy}	-7.2×10^5			
Luminosity, $cm^{-2}s^{-1}$	0.61×10^{35}	0.91×10^{35}	1×10^{35}	1×10^{35}

Interaction region optics, similar to SuperB, consists of separate chromaticity correction sections (sextupoles Y1 and Y3, X1 and X3) and crab sextupole (Figure 10). The optics also includes additional sextupoles Y2 and Y4, X2 and X4 to correct reduction of dynamic aperture due to finite length of main sextupoles [12], and sextupoles X5, X6, X7 help to correct nonlinear chromaticity [23,24].

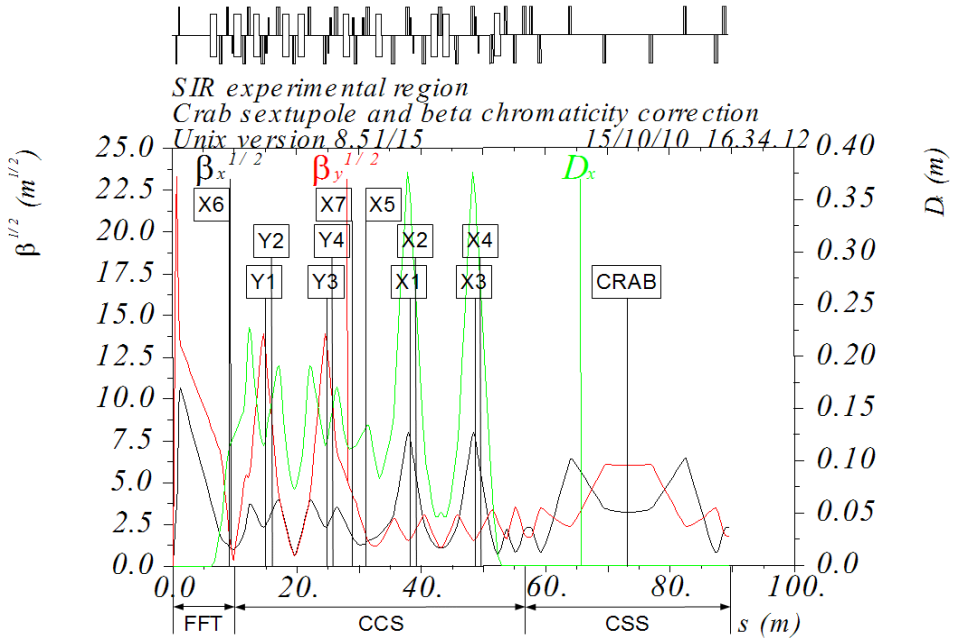

Figure 10: Optical functions of CTau interaction region.

3.3.5.3 *FCC-ee*

Future circular collider is a project in CERN of the next accelerator after LHC [25, 26]. The ultimate goal is 100 km proton-proton machine with 100TeV central mass energy. The first possible step is e^+e^- machine — FCC-ee with central mass energy range from 80 GeV to 350 GeV and two IPs (Table 4).

Table 4: Parameters of FCC-ee

	FCC-ee			
Experiment	Z	W	H	tt
Energy, GeV	45	80	120	175
Circumference, m	100×10^3			
$\varepsilon_x/\varepsilon_y$, nm/pm	0.14/1	0.44/2	1/2	2.1/4.3
β^*_x/β^*_y, mm	500/1			
Crossing angle, mrad	30			
σ_z, mm	5.9	9.1	8.2	6.6
Piwinski's angle φ	11	9	6	3
Beam current, A	1.4	1.4	0.3	0.06
Beam beam tune shift ξ_y per IP	0.175	0.187	0.16	0.08
μ'_y	-2805			
α^k_{yy}	4.5×10^5			
α^f_{yy}	1.9×10^5			
α^s_{yy}	-1.2×10^7			
Luminosity, $cm^{-2}s^{-1}$ per IP	211×10^{34}	36×10^{34}	9×10^{34}	1.3×10^{34}

Minimization of synchrotron radiation background towards the detector and the length of IR tunnel are important requirements; therefore, IR is asymmetric, i.e. with lower bending for the incoming beam and stronger bending for outgoing beam. Two teams developed different IR optics [27, 28].

The first variant (Figure 11) does not have horizontal chromaticity section because of geometrical constraints. The second sextupole of –I pair performs two functions: it cancels geometric aberrations of the first sextupole and, because dispersion is zero, it plays a role of crab sextupole. Individual –I pairs of arc sextupoles correct nonlinear chromaticity and dynamic aperture (Figure 12).

The second variant (Figure13) employs separate horizontal chromaticity corrections section and additional sextupoles as in CTau project. The arc sextupoles constitute two families. Dynamic aperture is comparable with the variant one (Figure14).

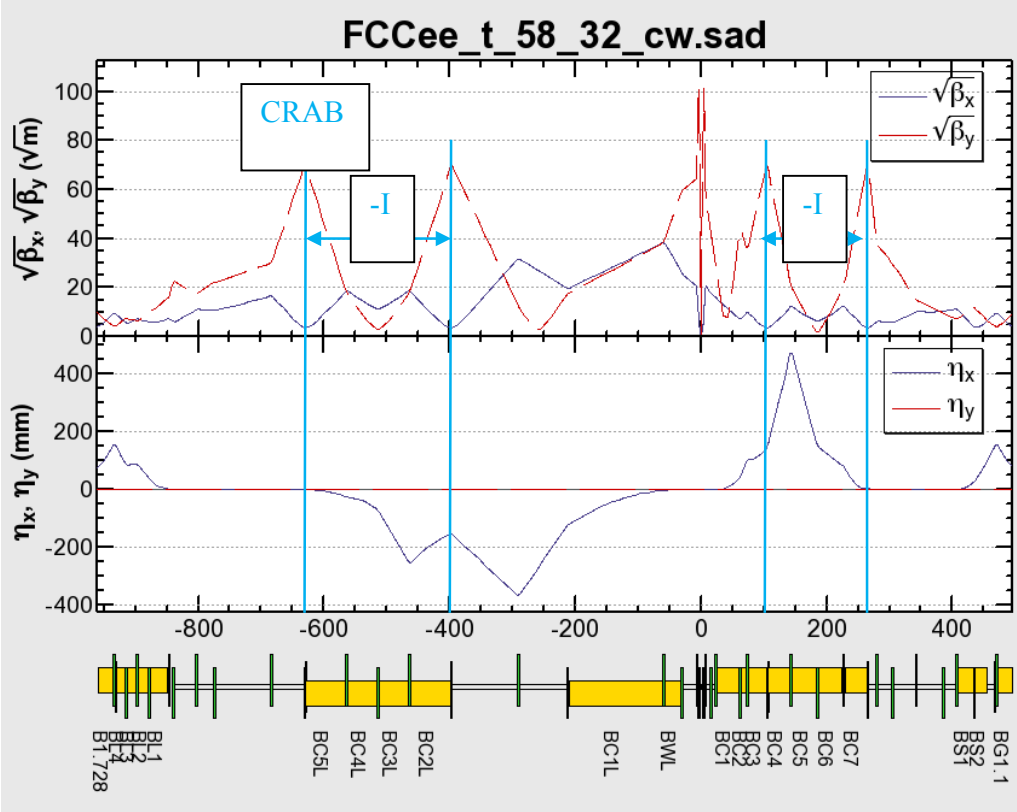

Figure 11: Optical functions of FCC-ee interaction region variant 1.

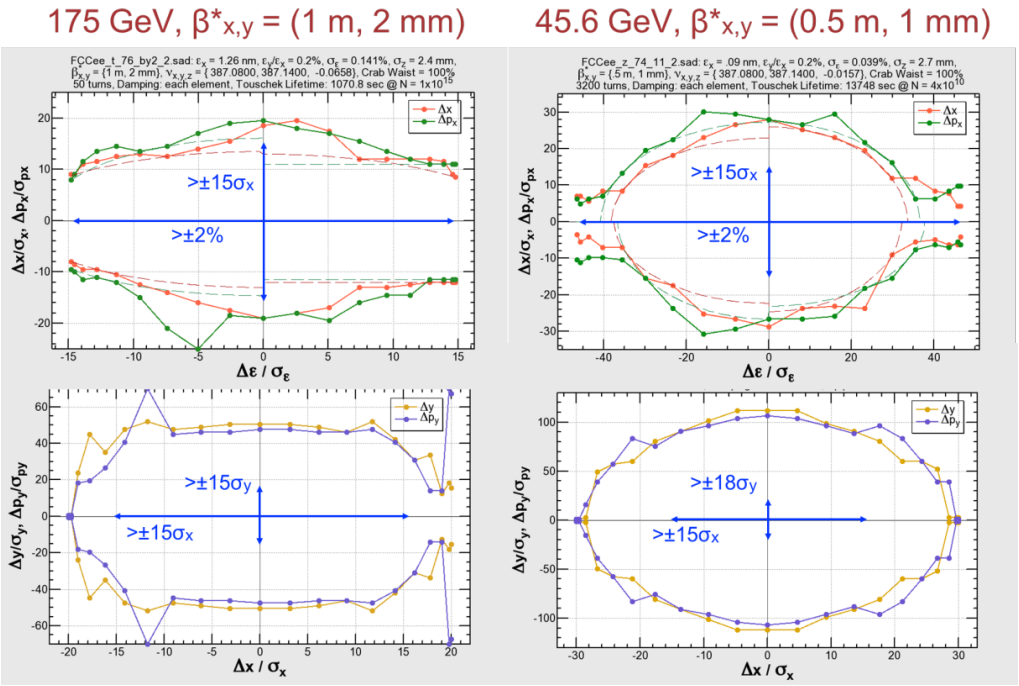

Figure 12: Dynamic aperture for FCC-ee interaction region variant 1.

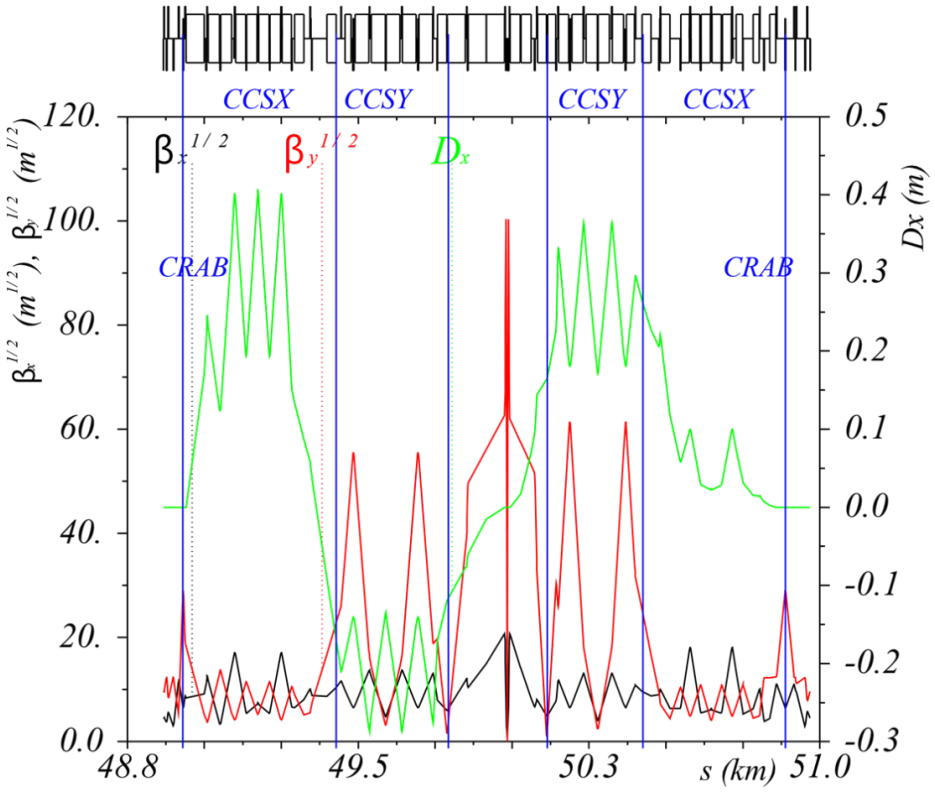

Figure 13: Optical functions of FCC-ee interaction region variant 2.

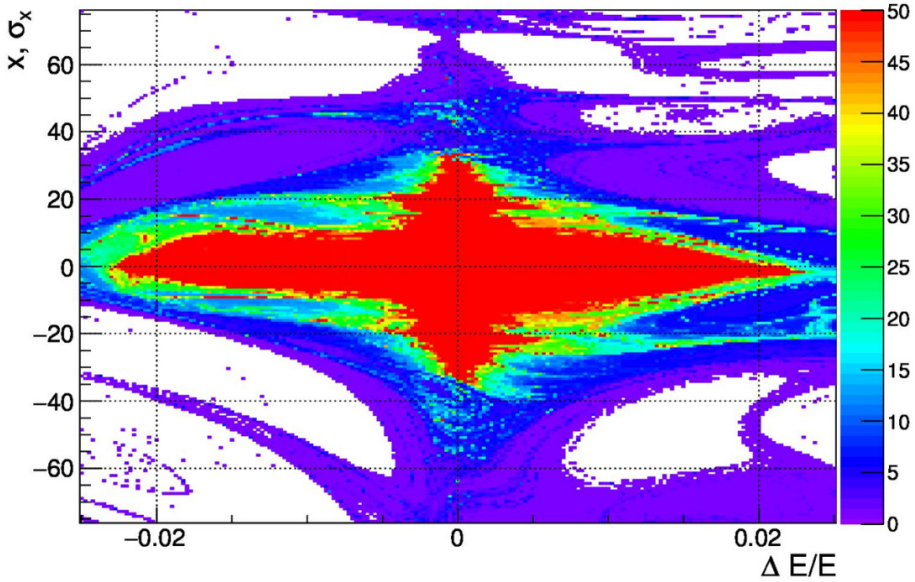

Figure 14: Dynamic aperture for FCC-ee interaction region variant 2 (50 turns, without damping, crab sextupole is off, RF is on).

3.3.5.4 *CEPC*

CEPC is Circular Electron Positron Collider in China [29, 30] with central mass energy range from 80 GeV to 240 GeV. The base line design is a single beam pipe collider with pretzel orbit scheme. In the base line design, it is not a high luminosity Z factory; therefore, the staff proposed partial double ring design [29] with crab waist collision scheme. The interaction region layout in the new proposal is similar to the second variant of FCC-ee.

3.3.6 **Discussion**

DAΦNE is the only collider among the reviewed projects, which does not report significant dynamic aperture loss from the crab sextupole. Observing detuning coefficients, we notice that SuperKEKB has the highest coefficients for kinematic term and for quadrupole fringe. The source of dynamic aperture reduction is then interference of crab sextupole with nonlinearities of kinematic terms and quadrupole fringes. To understand the nature of the dynamic aperture loss, we calculated the transfer map for a simple symmetrical case of thin crab sextupoles with strength ±K2L [m^{-2}], thin final quadrupoles with fringes K1L [m^{-1}] and K1 [m^{-1}], two drifts of the length L^* (from quadrupole to IP) with kinematic terms (Figure 15).

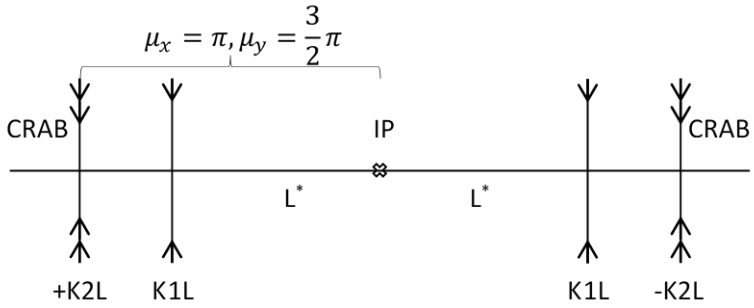

Figure 15: Layout of the simple interaction region.

Coordinates after the second crab sextupole depend on initial x_0, y_0 as

$$x = x_0 + y_0^4 \frac{L^*\left(1+2\cdot K1\cdot K1L\cdot L^{*3}\right)}{2\theta\beta_y^{*2}\beta_y^2}\sqrt{\frac{\beta_x}{\beta_x^*}} - x_0^4 \frac{K1\cdot K1L\cdot L^{*2}}{\theta\beta_y^*\beta_y}\sqrt{\frac{\beta_x^*}{\beta_x}} - x_0^2 y_0^2 \frac{L^*\left[\left(1+2\cdot K1\cdot K1L\cdot L^{*3}\right)\beta_x + 6\cdot K1\cdot K1L\cdot L^*\beta_x^*\beta_y^*\beta_y\right]}{2\theta\beta_y^{*2}\beta_y^2\sqrt{\beta_x^*\beta_x}}, \quad (13)$$

$$p_x = -x_0^3\frac{2}{3}K1\cdot K1L\frac{\beta_x^{*2}}{\beta_x^2} - x_0 y_0^2 \frac{2\cdot K1\cdot K1L\cdot L^{*2}\beta_x^*}{\beta_y^*\beta_y\beta_x}, \quad (14)$$

$$y = -y_0 - x_0^3 y_0 \frac{2\cdot K1\cdot K1L}{\theta}\left(\frac{L^{*2}}{\beta_y^*\beta_y}\sqrt{\frac{\beta_x^*}{\beta_x}} + \left(\frac{\beta_x^*}{\beta_x}\right)^{\frac{3}{2}}\right), \quad (15)$$

$$p_y = y_0^3 \frac{L^*\left(3+2\cdot K1\cdot K1L\cdot L^{*3}\right)}{3\beta_y^{*2}\beta_y^2} + x_0^2 y_0 \frac{2\cdot K1\cdot K1L\cdot L^{*2}\beta_x^*}{\beta_y^*\beta_y\beta_x}, \quad (16)$$

where we preserved the same notation for beta functions, and we chose $px_0=0$, $py_0=0$ for simplicity, and substituted crab sextupole strength (3). Introducing map notation V_{ijklm} for vector $z=\{x,p_x,y,p_y\}$ ($z_i=V_{ijklm}z_jz_kz_lz_m$), we compare the largest coefficients for different projects (Table 5). Again, we notice that SuperKEKB has the largest coefficient from the interference of crab sextupole and quadrupole fringe.

Table 5: Comparison of the map coefficients for different projects

	V_{11133}	V_{13333}
DAΦNE	$-3268-71\cdot K1\cdot K1L$	$3268+55\cdot K1\cdot K1L$
SuperKEKB	$-31481-51501\cdot K1\cdot K1L$	$31481+51465\cdot K1\cdot K1L$
SuperB	$-31849-2091\cdot K1\cdot K1L$	$31849+2087\cdot K1\cdot K1L$
CTau	$-64492-27894\cdot K1\cdot K1L$	$64492+27860\cdot K1\cdot K1L$
FCC	$-438-7063\cdot K1\cdot K1L$	$438+7011\cdot K1\cdot K1L$

Careful inspection of expressions (13, 14, 15, 16) shows that increasing vertical beta function β_y in crab sextupole decreases majority of the terms, thus providing a way to enhance dynamic aperture. Introduction of an octupole in the final quadrupole will provide the same monomials in the map; therefore, it is another way to optimize dynamic aperture.

3.3.7 Acknowledgements

We express our gratitude to Mikhail Zobov for details about DAΦNE upgrade.

3.3.8 References

1. P. Raimondi, “Status on SuperB Effort”, presentation at the 2nd Workshop on Super B-Factory, http://www.lnf.infn.it/conference/superb06/talks/raimondi1.ppt
2. M. Zobov, “New generation electron-positron factories”, Phys.Part.Nucl. 42: 782-799, 2011.
3. P. Raimondi and M. Zobov, DAΦNE Technical Note G-58, April 2003;
4. D. Shatilov and M. Zobov, ICFA Beam Dyn.Newslett.37:99-109, 2005.
5. A. Piwinski, “Satellite resonances due to beam-beam interaction”, IEEE Transactions on Nuclear Science, vol. NS-24, no.3, June 1977.
6. D.V.Pestrikov, “Vertical Synchrobetatron Resonances due to Beam-Beam Interaction with Horizontal Crossing”, Nucl.Instrum.Meth.A336:427-437, 1993.
7. P. Raimondi, D. Shatilov D and M. Zobov, “Beam-beam issues for colliding schemes with large Piwinski angle and crabbed waist”, Preprint physics/0702033, 2007.

8. P. Raimondi, D. Shatilov and M. Zobov, “Suppression of beam-beam resonances in crab waist collisions”, Conf. Proc. C0806233 WEPP045, 2008.

9. D. Shatilov, E. Levichev, E. Simonov and M. Zobov, “Application of frequency map analysis to beam-beam effects study in crab waist collision scheme”, Phys. Rev. ST Accel. Beams 14 014001, 2011.

10. A. Bogomyagkov et al., “Analysis of the Non-linear Fringe Effects of Large Aperture Triplets for the HL LHC Project”, Proceedings of IPAC2013, Shanghai, China, paper WEPEA049, pp. 2616-2617.

11. A.Bogomyagkov, E.Levichev, P.Piminov, “Nonlinear Perturbations for High Luminosity e+e- Collider Interaction Region”, IAS HEP Conference, 18-21 Jan 2016, Hong Kong.

12. A. Bogomyagkov, S. Glukhov, E. Levichev, P. Piminov. Effect of the sextupole finite length on dynamic aperture in the collider final focus, Arxiv: 0909.4872.

13. K. Oide, “KEKB B-Factory, The Luminosity Frontier”, Progress of Theoretical Physics, v. 122, p. 69, 2009.

14. T. Abeet al., KEK-REPORT-2010-1. 2010; arXiv:1011.0352.

15. Y. Ohnishi et al., “Accelerator design at SuperKEKB”,Progress of Theoretical Experimental Physics, 03A011 (17 pages), 2013.

16. Y. Funakoshi et al., “Beam Commissioning of SuperKEKB”, proceedings of IPAC16, tuoba01, http://www.ipac16.org, 2016.

17. Y. Ohnishi, “Optics Issues”, 18th KEKB Review KEK, March 3-5, 2014.

18. Y. Ohnishi, “Dynamic aperture optimization at SuperKEKB”, 55th ICFA Advanced Beams Dynamics Workshop on High Luminosity Circular e^+e^- colliders – Higgs factory, October 9-12, 2014.

19. Bona M. et al., Preprint SLAC-R-856, INFN-AE-07-02, LAL-07-15. 2007. 480 p.; hep-ex/0709.0451.

20. Biagini M. E. et al.,”SuperB progress report”, arXiv:1009.6178.

21. V. Anashin et al., “A project of super C-τ factory in Novosibirsk” conceptual design report, https://ctd.inp.nsk.su/c-tau, 2011.

22. Z. Zhou et al., “Preliminary concept and key technologies of hiepa accelerator”, proceedings of IPAC16, thpor047, http://www.ipac16.org, 2016.

23. R. Brinkmann, “Optimization of a final focus system for large momentum

bandwidth", Preprint DESY M-90-14, 1990.

24. A. Bogomyagkov, "Chromaticity correction of the interaction region", IAS Program on High Energy Physics, Hong Kong18-21 January, 2016.
25. M. Benedikt, "Future Circular Collider Study: status and parameter update", 2nd FCC week, Rome, http://fccw2016.web.cern.ch/fccw2016, 2016.
26. FCC-ee design study, http://tlep.web.cern.ch.
27. K. Oide, "Machine layout and beam optics", 2nd FCC week, Rome, http://fccw2016.web.cern.ch/fccw2016, 2016.
28. A. Bogomyagkov, "Interaction region optics solutions", 2nd FCC week, Rome, http://fccw2016.web.cern.ch/fccw2016, 2016.
29. D. Wang et al., "CEPC parameter choice and partial double ring design", proceedings of IPAC16, thpor010, http://www.ipac16.org, 2016.
30. Feng Su et al., "CEPC partial double ring lattice design", proceedings of IPAC16, thpor009, http://www.ipac16.org, 2016.

3.4 Introduction on the pretzel scheme design of CEPC

Huiping Geng

Mail to: genghp@ihep.ac.cn

Institute of High Energy Physics, 19B Yuquan Road, Shijingshan, Beijing, China

3.4.1 Introduction

After the discovery of Higgs-like boson at CERN[1,2,3], many proposals have been raised to build a Higgs factory to explicitly study the properties of the particle. One of the most attractive proposals is the Circular Electron and Positron Collider (CEPC) project in China[4,5].

CEPC is a ring with a circumference of 50-70 km, which will be used as electron and positron collider at phase-I and will be upgraded to a Super proton-proton Collider (SppC) at phase-II. The designed beam energy for CEPC is 120 GeV, the main constraints in the design is the synchrotron radiation power, which should be limited to 50 MW, the target luminosity is on the order of ~10^{34} $cm^{-2}s^{-1}$.

As beam energy is high, CEPC favors a lattice with more arcs which will enable RF cavities to compensate the energy loss in the straight section, thus can reduce energy variation from synchrotron radiation. SppC needs long straight sections for collimators etc. To compromise between CEPC and SppC, the ring is decided to have 8 arcs and 8